PROCEEDINGS, 51st Workshop on Geothermal Reservoir Engineering
Stanford University, Stanford, California, February 9-11, 2026
SGP-TR-230

Design Optimization of Metal-to-Metal Sealing Packers for Geothermal Operations through 3D-Printed Prototyping

Jose Aramendiz[1], Tayyab Shahid[1], Khizar Abid[1], Leonardo Rocha De Queiroz[2], Alberto Toledo Velazco[2], Satish Kumar[2], Yosafat Esquitin[2], Ricardo Reves Vasques[2], Ramadan Ahmed[1], Catalin Teodoriu[1].

[1]Mewbourne School of Petroleum and Geological Engineering, The University of Oklahoma, Norman, OK, USA

[2]Welltec Inc

cteodoriu@ou.edu

Keywords: Geothermal packers, Metal-to-metal sealing, 3D printing, Prototype optimization, Leakage analysis

ABSTRACT

Geothermal energy is not only a source of renewable energy but also has a low CO_2 footprint. However, the extraction of heat energy from the geothermal well comes with its challenges. One such challenge is the operation of the isolation tool in the geothermal downhole environment, where temperature and pressure are usually very high. The use of conventional oil and gas packers has limitations when installed in the geothermal well. Therefore, specific isolation tools must be designed to withstand harsh downhole well conditions and ensure long-term durability and integrity. In that respect, packers with metal-to-metal sealing are gaining importance for geothermal operations. However, the manufacturing of metallic packers is not only expensive and time-consuming, but also very demanding at the design stage. Therefore, it is preferable to develop small-scale prototypes, for which 3D printing can be a valuable tool to address design complexities, enabling rapid iterations and faster optimization. In that regard, Welltec designed a novel retrievable metallic packer and employed 3D printing to produce small-scale prototypes that allowed assembly evaluation and early detection of potential design challenges prior to full-scale manufacturing. This study presents the manufacturing and testing of different 3D designs prototypes that were designed, refined, and evolved based on performance feedback. The packer prototypes were printed using polylactic acid (PLA) and thermoplastic polyurethane (TPU) filaments and tested in a novel flow-by setup using translucent polyvinyl chloride (PVC) pipe as a wellbore. Vegetable glycerin (VG) mixed with propylene glycol (PV) in liquid form was vaporized to simulate the working fluid while high-speed video cameras recorded the process. In order to detect the leakage pathways, colored powder spray was utilized, which helps to analyze the fluid bypass and assist in analyzing sealing efficiency during tests. Additionally, differential pressure measurements provided insights into the sealing performance as the design cycle progressed. Overall, rapid prototyping with 3D printing demonstrated that iterative design process and component refinements can improve sealing capability at a small scale, providing critical insights to guide cost-effective development of field-scale metallic packers for geothermal applications.

1. INTRODUCTION

The global energy matrix is rapidly changing, driven by environmental concerns about the impacts of fossil fuels on the planet and human well-being. Between 2010 and 2023, CO_2 emissions increased from 32.8 to 37.7 Gt (IEA, 2024). Thus, energy transition towards different types renewable resources (i.e., solar, wind, geothermal, tide, etc.) have being a priority within the United Nation's Sustainable Development Goals (R.V et al., 2023), with renewables expected to increase their share of the global energy supply from about 12% in 2023 to 18% by 2030 and nearly 30% by 2050 (IEA, 2024).

In this context, geothermal energy has demonstrated significant potential as a sustainable alternative due to its low environmental footprint, reliability for continuous load operations, and independence from meteorological conditions (Qiao et al., 2024). Geothermal energy is a renewable resource stored in the form of heat within the Earth's crust and exploited by producing geothermal reservoir fluids to the surface through wellbores (Sharmin et al., 2023).

Despite its significant benefits and potential, geothermal energy currently has a limited share in the global energy generation, accounting for only 0.35 % (IEA, 2024; Nkinyam et al., 2025), primarily due to high initial investments and the challenges associated with drilling and completion operations under extreme working scenarios, where temperatures can reach up to about 400°C for enhance geothermal systems (EGS) (Roy et al., 2023).

Geothermal harsh downhole conditions are not limited only to temperature. Corrosive reservoir fluids are present (Arias et al., 2024) and high-pressure ratings are required to fracture high-strength rock formations in geothermal reservoirs (Hongwei et al., 2024). The combination of these unique conditions often exceeds the operational range of most conventional downhole tools, leading to failures and, subsequently, risks to well integrity (Song et al., 2023).

In the specific case of EGS, effective zonal isolation tools are crucial to guarantee the reliability of the operation while simulating and later on to keep an effective seal throughout the injection and production stages. Due to the lack of specific tools designed for geothermal wells, conventional elastomeric packers have been deployed in geothermal wells, however, most elastomers tend to fail as temperature conditions exceed 150 °C, leading to seal degradation (Li et al., 2024; Patel et al., 2019). An example of this was experienced- by the Frontier Observatory for Research in Geothermal Energy (FORGE) in the FORGE 58-32 injection well, in which multiple modes of packer failures were reported (McLennan & Podgorney, 2019).

In this context, Welltec has designed a metallic expandable packer (MEPs) for zonal isolation in EGS (Abid et al., 2022; Baena Velasquez et al., 2024). This system have been tested at High-pressure, High-temperature (HTHP) conditions (up to 6000 psi and 310°C) in a dedicated testing facility at the University of Oklahoma (Paba Vega et al., 2025) and have demonstrated their seal integrity under different conditions (Alvarez Escobar et al., 2025) supporting the potential of MEPs to be a dedicated solution for geothermal wells to guarantee their well integrity.

Conventional manufacturing methods for fabricating tools are time-consuming, and as model complexity increases or customization is required, costs rise sharply before an optimal, functional model is achieved. This is particularly critical because the cost is not limited to the time and energy spent during manufacturing but also includes the amount of raw material required and its cost (Allouzi et al., 2020; Burns & Wangenheim, 2019; Zhong et al., 2017).

In this respect, 3D printing also known as additive manufacturing (AM), is an innovative technique that can create objects by depositing material layer by layer rather than subtracting it, as in traditional methods (Sireesha et al., 2018). AM not only reduces costs but also shortens prototyping time, as it enables the fabrication of complex geometries and allows fine-tuning of special features in the model, facilitating rapid iteration and optimization of the final product that would not be feasible or cost-effective with conventional techniques (Lemu, 2016; Tavares & Aldakhil, 2024; Vasquez, 2020).

The application of AM in the energy sector has gained traction in recent years, with several successful applications reported in the literature. These include backup ring elements for downhole packers in oil and gas (O&G) (Deng et al., 2018; Green et al., 2024) and geothermal wells (Krumm et al., 2021), flapper valves (Burns & Wangenheim, 2019), prototypes of petal-type expandable packers (Zhong et al., 2017), lost-circulation materials (Hitchcock & H. Arfarj, 2024), wedge-wire laterals for sand filters (Banna et al., 2024), hydrocyclones (Zhao et al., 2024), asset protection and spare parts (Tavares & Aldakhil, 2024), and samples for fracture conductivity tests (White et al., 2024).

While Welltec's MEPs have already shown success in geothermal (Welltec, 2026.) and O&G applications (Ali et al., 2023), the system was designed as a permanent packer solution. Leveraging this experience, Welltec is designing and evaluating the feasibility of deploying a retrievable system, with a metal-to-metal sealing mechanism, that can withstand geothermal downhole conditions, specifically those encountered at the FORGE site project.

Although some of the technology foundation from the permanent packer can be transferred to this new concept, the system's retrieval nature introduces unique design and mechanical complexities, particularly in tolerance and sealing interactions among individual features. To address these challenges, an iterative and flexible design approach was considered, where evaluation and fine-tuning of critical features could be performed in an efficient manner without involving large-scale manufacturing models. Thus, AM was adopted as a key tool to develop multiple small-scale prototypes, allowing rapid design iterations and refinements as well as detecting early design challenges of the packer concept based on feedback from the evolution process, providing valuable insights prior to full-scale manufacturing and testing.

This study presents the application of AM as a design tool to reproduce 3D-printed small-scale packer prototypes and the methodology followed to support fine-tuning adjustment to develop the concept of a retrievable metallic packer for geothermal applications.

2. MATERIALS AND METHODS

The experimental design discussed in this study was derived from a series of flow tests to characterize the seal behavior of small-scale 3D-printed packer prototypes and to identify features that required fine-tuning to optimize the proposed models. Figure 1 presents a flowchart of the proposed methodology.

A 3D printer with fused deposition modelling (FDM) technology (i.e. Bambu Lab X-1 carbon) and a bed size of 256 mm x 256 mm x 256 mm was used to create the packer prototypes. The printer employs features such as LiDAR sensors, dual-bed leveling, and compensation for vibration and extrusion, ensuring precision and reliability. The printer operates with a layer resolution in the range of 0.01 to 0.3 mm with a position accuracy of 7 µm in the X/Y direction and 0.05 µm in the z-direction. A 0.4-mm-diameter copper nozzle was used for all prints. The nozzle and bed temperatures were maintained between 200–235 °C and 58–60 °C, respectively, depending on the filament type.

For this specific study, PLA filament with a density of 1.24 g/cc was used to print all structural components of the prototypes. Its excellent printability enabled smooth layer adhesion and a high-quality surface finish. TPU filament with a density of 1.24 g/cc and a hardness of 95A was employed for selected sealing elements in prototypes requiring increased flexibility. All filaments used in this study have a nominal diameter of 1.75 mm and were air-dried for at least 12 hours at 50°C before printing to remove moisture.

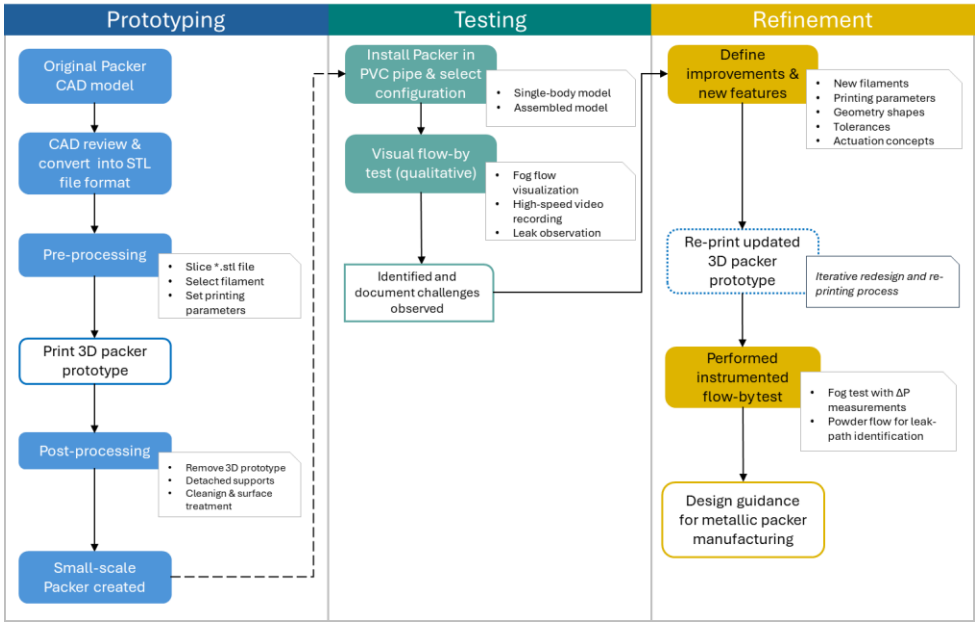

Figure 1: Flow chart of the proposed methodology.

Two software applications were used during the design and manufacturing stages, as summarized in Table 1.

Table 1: List of Software used in the 3D project.

SOFTWARE	DESCRIPTION	PURPOSE
Autodesk Fusion	A cloud-based 3D CAD, CAM, and CAE tool that integrates design, engineering, and manufacturing processes into a single platform.	Used to review the original CAD geometry, split the single-mesh body into multiple components when required, and export STL files.
Bambu Lab Studio	Slicing software developed for Bambu Lab 3D printers, providing advanced slicing features and customizable print profiles for different materials.	Used for slicing objects to be printed with the Bambu X-1 Carbon as well as optimizing specific print settings

2.1 3D printing procedure and settings. Printing parameters were selected to ensure dimensional consistency and minimize surface discontinuities along critical parts. All components were printed using a layer height of 0.15 mm and a two-wall line count. The infill density was set to 15% with a grid infill pattern applied across all structural components. Printing orientation was selected based on the functional requirements of the printed components. Tree support structures were generated for overhang angles > 60°. An overall print speed of 200 mm/s was used, with reduced speeds (<50 mm/s) applied only when printing selected TPU components to ensure print stability.

After printing, standard post-processing steps were applied when required to prepare the prototypes for assembly and testing. Support material was removed, and minor surface imperfections were corrected using fine-grit sandpaper and files, if needed, with special care in regions associated with sealing contact. Printed models were either stored as single-body packers or assembled part by part into the respective packer prototypes and then stored with desiccant to minimize moisture absorption prior to testing.

2.2 Flow-by Test Setup. The setup configuration, shown in Figure 2, was built at the Well Construction Technology Center (WCTC) at the University of Oklahoma to qualitatively evaluate the sealing behavior of the packer prototypes. The system consisted of a vertical transparent 4-in PVC pipe section for packer installation, a fog chamber, a variable-speed fan at the bottom, and a portable vacuum at the top to control fog flow.

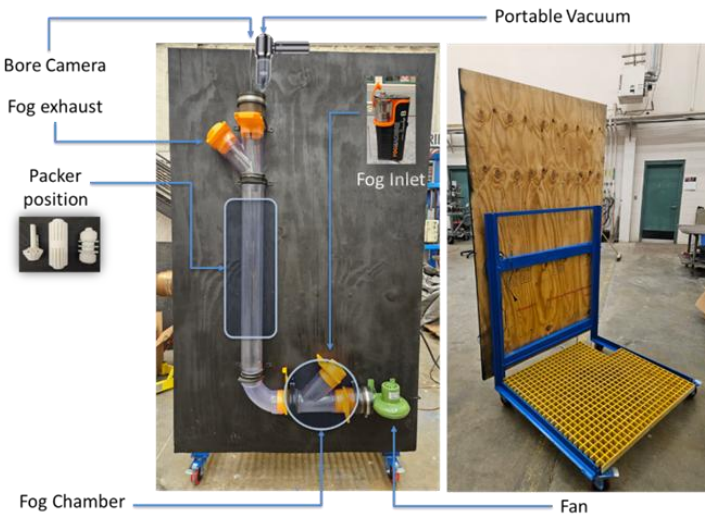

Figure 2: Flow by test configuration.

Fog was generated using a LESONG smoke B (Figure 3A) machine to simulate steam. This equipment is a portable device that can produce enough fog to cover 20 cubic meters per minute, using a non-toxic vegetable glycerin and propylene glycol fluid. The fog flows in a bottom-up configuration, and internal and external cameras seen in Figure 3B, were used to record flow behavior and potential leakage paths, with frame rates in the range of 30-800 fps.

Figure 3: Lesong smoke B fog machine (A) & set of cameras to record flow behavior (B).

2.3 Flow-by test procedure. The flowchart shown in Figure 4 outlines the step-by-step process established for the flow by test. The process can be divided into four main steps: Packer installation, fog chamber filling, flowing test, and finally, video editing and evaluation.

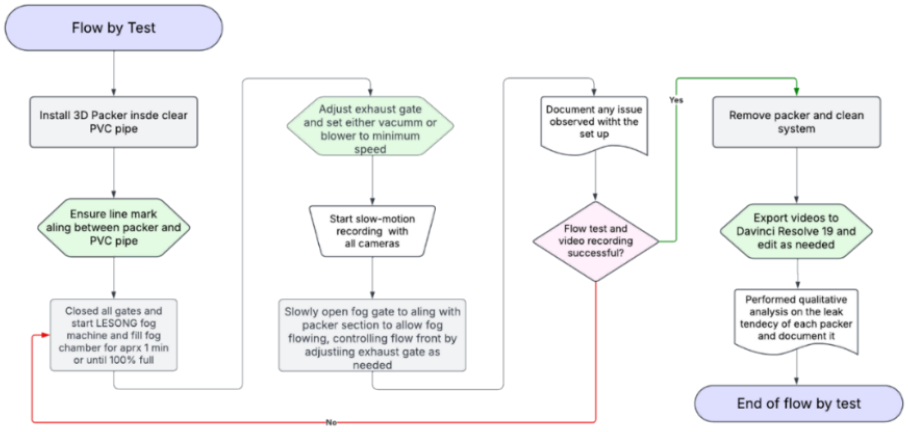

Figure 4: Flowchart of flow by test.

This first test enables a qualitative assessment of the packers' sealing performance, highlighting key challenges and observations related to the design, the filament material, or the deployment mechanism. The shorter the time the fog takes to pass through the packer's seal section, the faster the upper portion of the PVC pipe is filled, which was used as an indicator of sealing efficiency.

2.4 Differential pressure test. This second test included an Eaton digital manometer featuring a dual-port configuration for differential pressure measurements, with a full-scale range of 3 psi (83.02 inH2O) and a resolution of 0.001 psi (0.01 inH_2O). This analogy applies to our setup: if there is no seal, there will be no reading, an indication of a 100% leak. As the packers' sealing improves, the differential pressure readings will increase. Figure 5 shows the updated version of the setup, including the manometer.

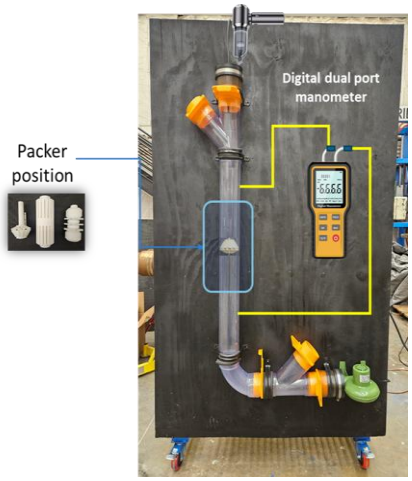

Figure 5: Flow-by test configuration with digital manometer.

To establish a baseline for the differential pressure measurements, a PLA disc with an ID slightly larger than that of the PVC pipe was printed (Figure 6). The disc was installed in the PVC pipe. The fan was turned on, and differential pressure readings were gathered at the minimum and maximum speed. The same procedure was followed to measure the sealing capability of different packer prototypes, and the measurements were compared to the baseline obtained with the reference disk for quantitative seal analysis.

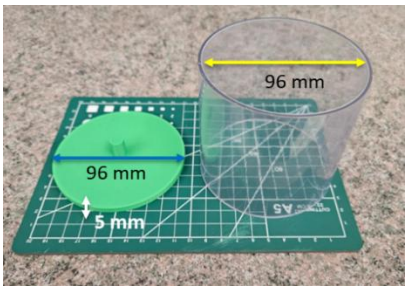

Figure 6: PLA reference disc for differential pressure measurements.

2.5 Powdered fog test. The objective of this test is to identify potential leak paths along the seal section of the packer prototype. To accomplish this, a red powdered spray was flowed through the packer deployed inside the flow-by setup. The red particles contained in the spray filled areas or sections prone to leakage. The larger the leak area, the more particles will be deposited. Figure 7 shows the powdered spray used in this test.

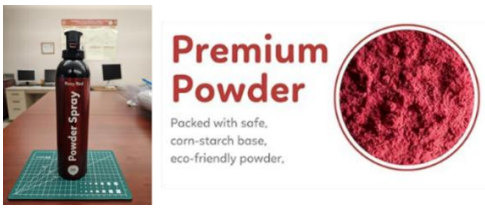

Figure 7: Red powdered spray to detect leak zones.

3. RESULTS AND DISCUSSION

Three main tasks were conducted to evaluate the 3D models, starting with prototyping and printing. Flow-by tests were then conducted on the models. Based on initial results, adjustments were made, and, finally, differential pressure and fog tests were performed as the final step in 3D model characterization.

3.1 1st Iteration results and analysis

In this step, the baseline models consisted of prototypes printed using PLA filament, with all of them in the set position. This approach gave the team a first insight into how the models looked when deployed and the potential interaction against the PVC walls of the pipe used to simulate the wellbore. Figure 8 shows the HEX (left), the keystone (center) and the OU packer model (right) with the discs also printed with PLA.

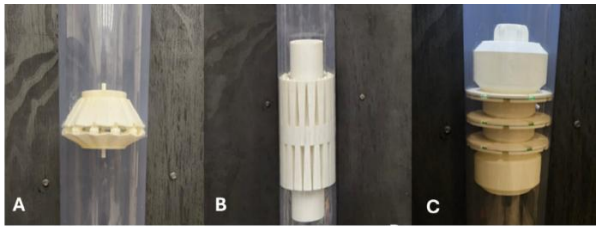

Figure 8: HEX model (A), Keystone (B), OU Packer (C).

The first packer tested was the HEX. An advantage of this packer is that the space between the links is eliminated when printed as a single body. This forces the fog to flow directly to the contact area between the edge of the petals and the wall of the PVC pipe. Figure 9 illustrates a sequence of 11 seconds from a front-facing video recorded at 30 fps. The seal barely manages to contain the fog below the packer. It took only 2 seconds for the leak to initiate and 3 more seconds for the seal to completely lose its integrity.

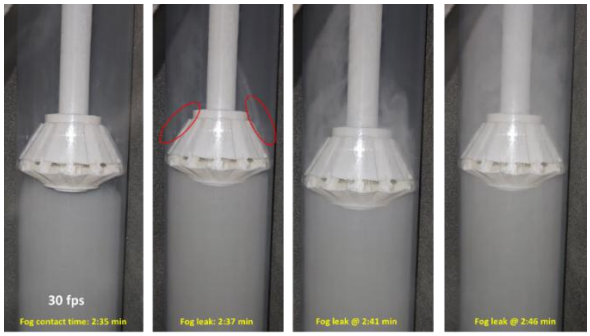

Figure 9: Front-view video sequence of HEX packer.

Figure 10 shows a sequence from the side-view camera in slow motion using 240 fps. The duration may appear longer; however, this is mainly due to the higher frame rate used. This image is intended only to highlight the sections where the leak initiates. In this specific sequence, it was possible to adjust the contrast to visualize the fog in red tones, which helped identify the areas where the leak began.

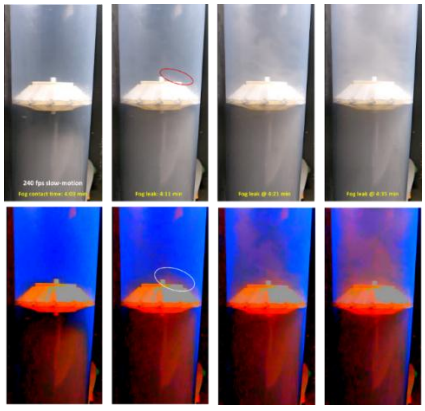

Figure 10: Front-view video sequence of HEX packer.

The keystone model was the second tested. The entire model was printed as a single body; however, the boundaries between fingers still show signs of separation, which may explain why the leak began roughly 2 seconds after the test started, despite the extended sealing length. Figure 11 shows the front-view video sequence. It is important to note that the video was recorded at 240 fps, so the visual timeline does not correspond to real-time seconds. Therefore, the moment of leak initiation observed in the footage does not correspond to the actual time progression at the second level.

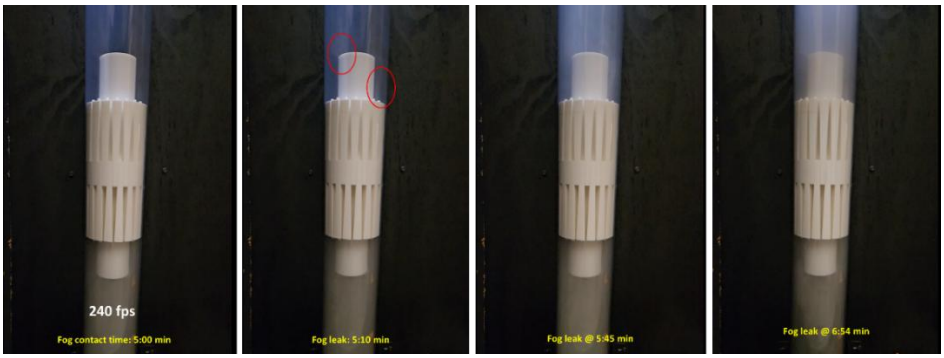

Figure 11: Front-view video sequence of Modified Packer.

Based on this initial outcome, the team concluded that, for the 2nd iteration, improvements should either adjust the finger geometry or evaluate alternative filaments and actuation mechanisms to achieve a stronger seal that better conforms to the inner wall of the PVC pipe.

The OU packer consisted of three seal elements resembling discs in series. Based on the lessons learned from the HEX, a main pipe with grooves was used so that all elements could slide linearly. The leak started very quickly after the fog first contacted the bottom section of the packer, this time even faster than with the HEX, with the leak starting in about 2 seconds and becoming fully developed in less than 4 seconds. Still, the overall results were similar to the Keystone. Figure 12 shows the front-view video sequence.

From the video analysis, it could be seen that the right section of the packer filled faster than the left side. It was hard to observe clearly, but there was likely a leak between the inner section of the discs and the main pipe. As a result, the model may require adjustments in that area to reduce the impact of components unrelated to the seal section on leak performance.

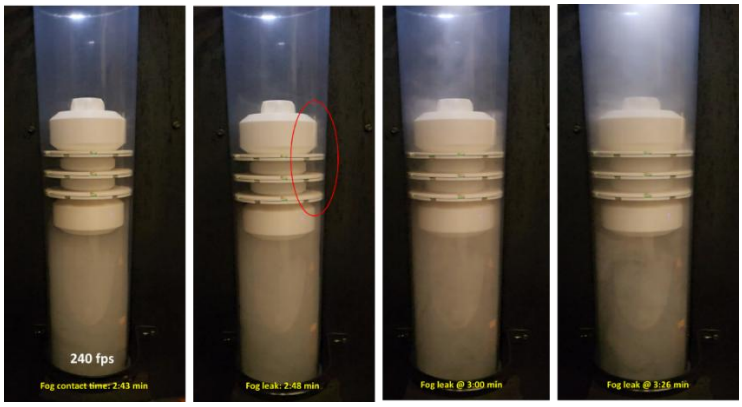

Figure 12: Front-view video sequence of OU Packer.

Overall, the results of the 1st iteration showed that fog easily breaks through the seal of all packers. This highlighted the need to adjust the sealing elements and to incorporate an actuation mechanism that more accurately simulates real-world operations to improve the testing approach. Regarding filament selection, PLA, being a strong plastic material, provides good infill density for the packer structure. However, its impact on the seal elements could be negative, as it may reduce conformance with the PVC walls, preventing the packers from achieving a higher seal. Reducing some rigidity of the filament material used for the seal sections may enhance the seal element's conformance against the pipe walls, creating a more effective seal and reducing potential leakage.

3.2 2nd Iteration results and analysis

In this step, the prototypes were 3D-printed using the PLA filament for the body structure and TPU for the sealing components. The process required printing the packers as separate elements and then assembling them together; in the case of the Keystone, it also incorporates the actuation system that will deploy the packer inside the PVC pipe. This round only focused on the keystone and the OU packer models, as the HEX was oriented for casing applications and the other for open-hole retrievable conditions.

The first attempt for the keystone option considered printing the base pipe, the movable parts, and the fingers individually. Three 2-mm-diameter holes were drilled in the lats to accommodate a 16-caliber wire for securing the lats around the base pipe. However, this approach was unsuccessful, as shown in Figure 13.

Figure 13: Keystone blade failure.

The evolution of the Keystone then required creating a system capable of dynamically moving a group of fingers, installed on a crown element on each side of the system, along a linear path. A seal is formed when the fingers meet in the center. Figure 14 illustrates the initial version of the keystone with this system, using a hinge to connect the fingers to the crown. The challenge with this system was to keep the finger in place, since there was no locking mechanism, it moved uncontrollably inward or outward.

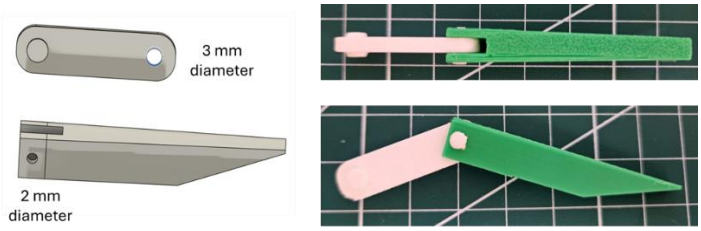

Figure 14: Keystone hinge-finger 1st configuration.

In the 2nd iteration, the finger shapes were shortened, and a smooth curvature was introduced to better conform to the PVC walls. The hinge system was changed, adding a locking mechanism on each side to keep them straight and only moving linearly with the actuation system. Figure 15 shows the refined finger features. This system has become the base design for the potential retrievable metallic packer to be manufactured in later stages.

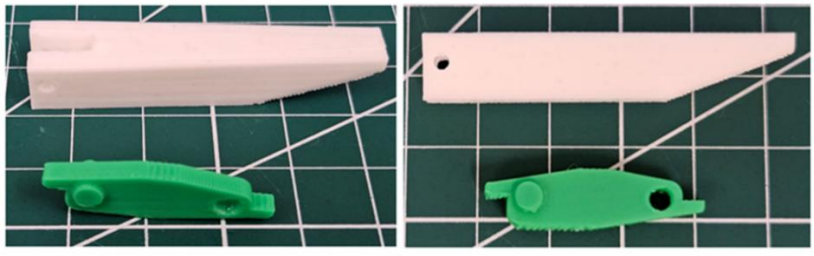

Figure 15: Keystone hinge-finger 2nd configuration.

Figure 16 illustrates the difference between the 1st and the 2nd finger-hinge configuration. It is evident that the new lock mechanism helps keep the finger straight, while the 1st model experiences an inward motion. Figure 17 shows the 3D model printed with the 2nd finger configuration, while Figure 18 shows the entire Keystone CAD model.

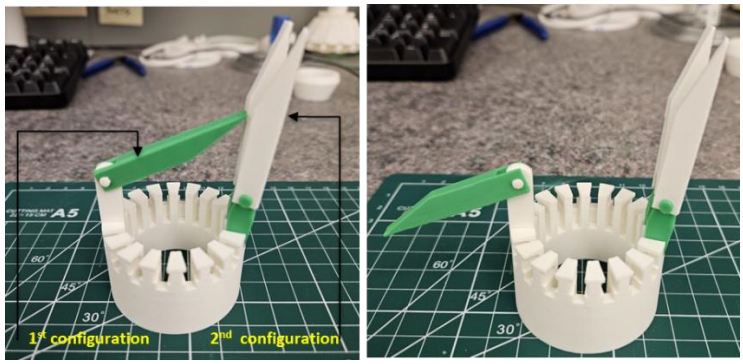

Figure 16: Keystone configurations comparison.

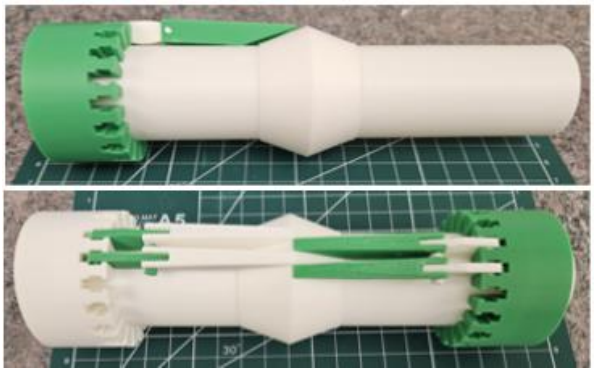

Figure 17: Update 3D printed keystone concept.

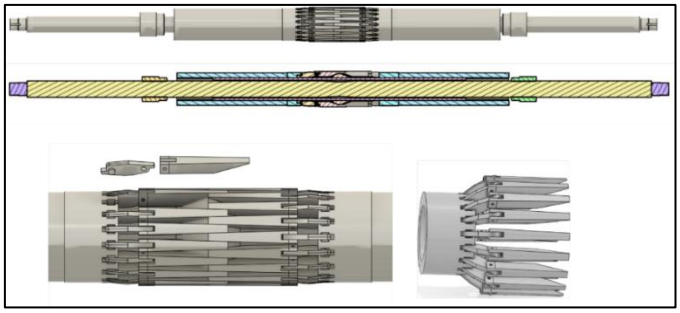

Figure 18: Update 3D printed keystone concept.

The main changes in the Keystone model rely on a new short link that connects the individual fingers to the crown. The features at each end prevent the fingers from moving uncontrollably inward or outward. In this updated model, only the fingers were printed in TPU with high infill density, while the remaining components were printed in PLA. Once the small parts were solved, the challenge shifted to the larger elements, more specifically, the base pipe and the movable elements. Guides and grooves were needed on both components. This step was vital to ensure that when the actuation system was integrated into the packer, and both sides of the system moved simultaneously with no rotation or additional torque added.

For the OU packer, movable cylinders that push the ring seal elements were printed separately. A rail and groove (within the base pipe), and the seal rings were designed to avoid rotation while running it into the PVC pipe. Figure 19 shows the movable body and the base pipe.

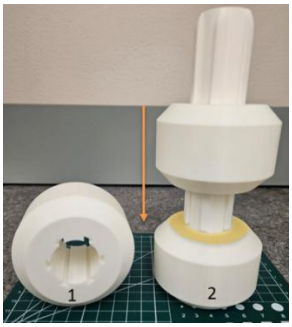

Figure 19: Movable elements in OU Packer.

For the discs, TPU filament was considered. Initial prints showed bad surface results on the disc's surfaces due to moisture. Thus, the filament was dried for 12 hours at 50°C before printing. Additionally, to improve surface finish and reduce layer adhesion, the nozzle temperature was reduced from 240°C to 235°C, and the printing speed was reduced by 60–70% relative to PLA. Figure 20 illustrates the improvement in print quality from left to right after incorporating the drying step. This step helped to resolve the surface finish issues.

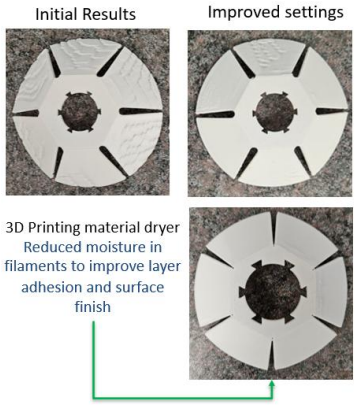

Figure 20: TPU disc evolution varying printing settings.

The actuation mechanism designed for the Keystone included a bi-directional lead screw with two pushing plates. Each pushing plate is connected to the end of the PLA movable element. This mechanism would linearly displace the movable components of the packers without rotation and finally compress the seal elements against the PVC pipes, creating the seal. Figure 21 illustrates the actuation mechanism, while Figure 22 shows the mechanism deployed within the PVC pipe, with a seal section of approximately 28 mm.

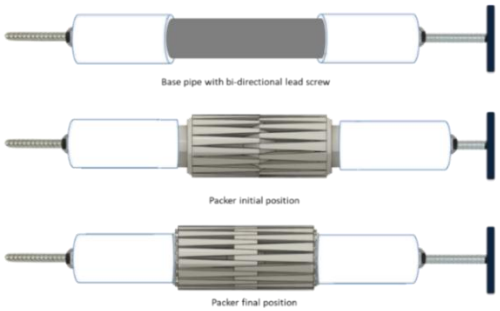

Figure 21: TPU disc evolution varying printing settings.

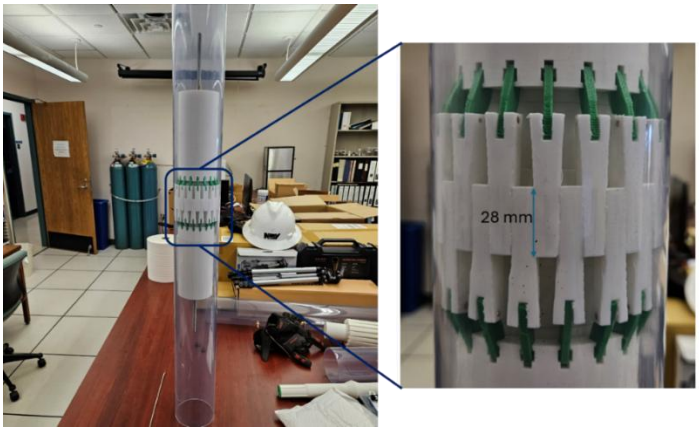

Figure 22: 3D deployment test of Keystone prototype.

With these refinements, differential pressure and fog tests were carried out to evaluate the new models' sealing characteristics.

3.2.1 Flow-by tests results

Figure 23 illustrates a sequence of 10 minutes and 4 seconds (1 minute and 15 seconds at normal speed) for the Keystone model from a front-facing video recorded at 240 fps. It was observed that the leak initiated in the right-back zone of the prototype. Interestingly, the fog created a kind of static wave on the front-left side, which gradually evolved into a slope as it moved to the right.

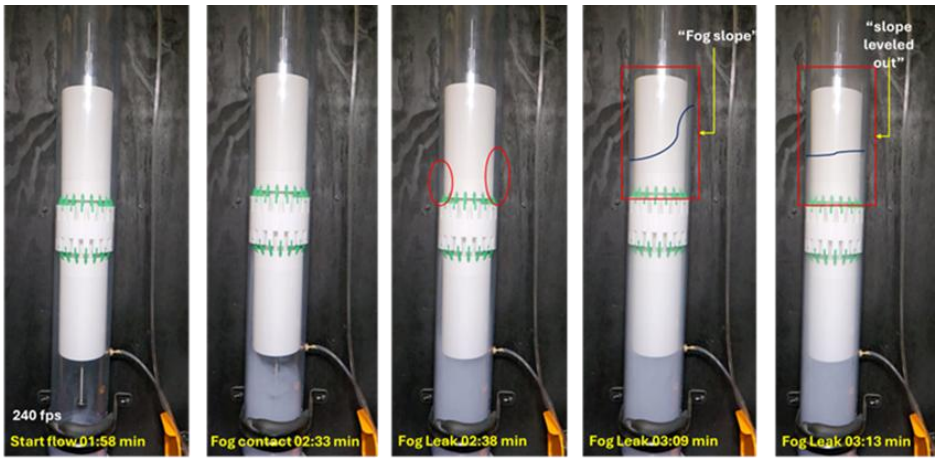

Figure 23: Front-view video sequence of Keystone Packer.

As the leak progressed and more fog volume accumulated above the seal zone, the slope leveled out, and a uniform leak front developed. This fog slope was not seen in previous packers. If individual finger positions can be adjusted, a more uniform sealing could be achieved, improving how the packer controls the leak tendency. This gave important design consideration to the team as for the retrievable metallic model, individual movements of the fingers should be considered to create a more effective seal zone.

It is important to note that the video was recorded at 240 fps, so the visual timeline does not correspond to real-time seconds. Therefore, the moment of leak initiation observed in the footage does not correspond to the actual time progression at the second level. However, it was estimated from a series of tests that the seal lost its integrity in approximately 8 seconds.

In the case of the OU packer, the leak still started quickly after the fog first contacted the packer, as experienced in the 1st iteration. However, with the discs printed in TPU leak fully developed in about 6 seconds, a difference of 3 seconds compared to the PLA model. Figure 24 shows the side-view sequence of the flow-by test. It was observed that the front-section of the packer leaked faster than the back section.

It was difficult to observe clearly, but there was still a leak between the inner sections of the discs and the main pipe, indicating that this issue may become a major and difficult challenge to address if it progresses to the next manufacturing stage. Nevertheless, one potential design improvement to address this condition is to reduce the spacing between pairs of discs and increase their number, thereby increasing the effective seal area against the PVC walls and potentially improving the packer's seal control.

.

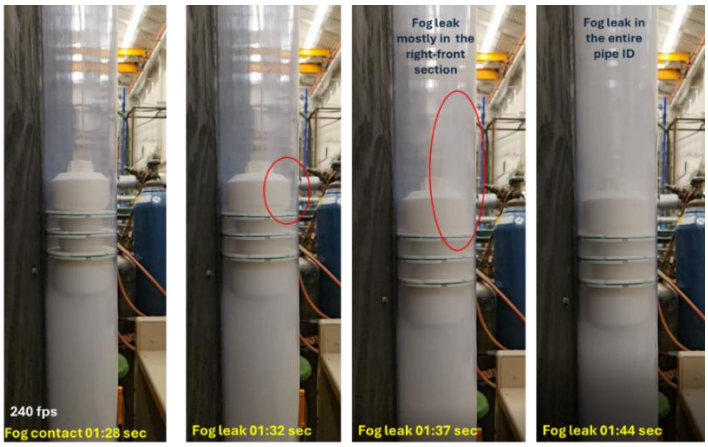

Figure 24: Side-view video sequence of the OU packer with TPU discs.

3.2.2 Differential pressure test results

The process of obtaining the differential pressure measurements began with the readings of the reference disc. Figure 25 shows the results for the reference disc, at the minimum fan speed, the results varied from 0.19 to 0.20 inH_2O, whereas at the maximum fan speed, the results stabilized at 2.06 inH_2O.

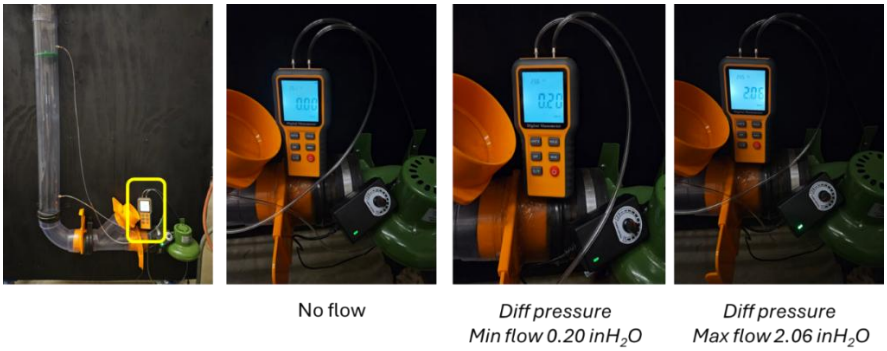

Figure 25: Reference disc differential pressure measurements.

The data obtained using the disc reference were used for comparison with the other 3D packer prototypes. As a reference Figure 26 shows the test performed with the Keystone packer prototype.

Figure 26: Differential pressure measurements for Keystone assembled model.

Table 2 summarizes all the results. The best seal performance compared to the reference disc was the HEX module, which experienced only a 0.48% drop in differential pressure. OU packers with PLA discs and Keystone single body experienced a drop in sealing

performance of 9.22% and 14.07% respectively, under maximum flow. Differential pressure at minimum fan speed for all models was within the range obtained for the reference disc.

Table 2: Packer prototypes differential pressure measurements.

Packer Prototype	Differential pressure Min flow (inH_2O)	Differential pressure Max flow (inH_2O)	Sealing capability drop at Max flow (%)
Reference Disc	0.19-0.20	2.06	NA
HEX	0.2	2.05	0.48
Keystone (single-body)	0.19	1.77	14.07
OU Packer (PLA)	0.2	1.87	9.22
OU Packer (TPU)	0.19	1.99	3.4
Keystone (assembled)	0.19	1.90	7.77

One of the disadvantages of the single body models printed with PLA filament is that the conformance to the PVC walls is affected as not much torque or pressure could be applied before they break and thus, at least, a degree of flexibility may be needed to obtained a more representative conditions for the sealing structure. Therefore, when the sealing elements of both the OU and the keystone models were printed with TPU filament, the edge of the elements tends to conform much better to the irregularities of the PVC walls, generating a better seal.

The differential pressure results of these two models support this claim. At maximum flow OU Packer with TPU discs exhibited a differential pressure drop of 3.40 % compared to the reference disc but improved the sealing capability by 6.42% when compared to the OU Packer with PLA discs, which indicates that the material used to print the sealing elements plays a considerable role in the final performance of the packer. Keystone prototype with fingers printed in TPU experienced a drop in differential pressure of 7.77% compared to the reference disc but improved its seal capability by 7.34% compared to the Keystone printed as a single body in PLA filament.

Although it is difficult to evaluate minor irregularities within each model that may increase the leak, the results present the overall leak behavior of the system. Still, there were certain conditions that were identified that may be connected to leak tendencies. For example, Figure 27 illustrates small opening zones between the fingers and the top of the triangle on the base pipe that may affect seal performance.

Figure 27: Potential leak spot in Keystone assembled model.

Identifying conditions such as these is one of the objectives of the proposed methodology, as it enables the rapid AM process to reveal potential issues that the metallic packer may experience. This, in turn, gives design engineers the opportunity to fine-tune critical components and make informed design changes prior to deciding which model should be passed to the next phase of manufacturing.

3.2.3 Powdered fog test results

The powdered red spray flowed through the OU TPU and the keystone packer prototype. The following figures depict the potential leak paths for each system. Figure 28 illustrates the OU TPU packer. It was observed that the leak path develops in a spiral pattern due to the

petal design, as indicated by the yellow arrows. One main reason is that the prototype packer lacks an actuation system capable of inducing higher stress at the edges of the sealing elements and the PVC walls.

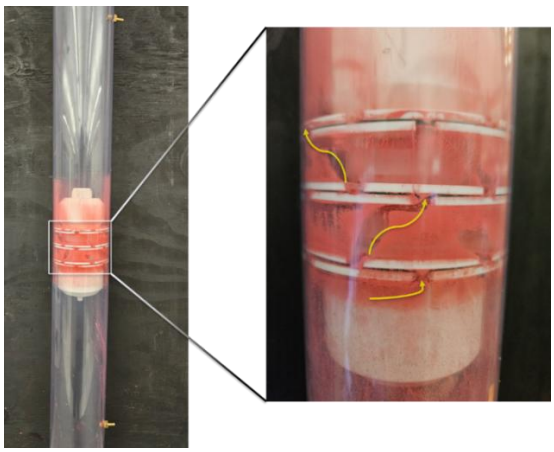

Figure 28: OU TPU packer powdered leak path results.

Figure 29 shows the results for the Keystone prototype. With this system, it could be noted that three conditions lead to the leakage path to develop, which are as follows:

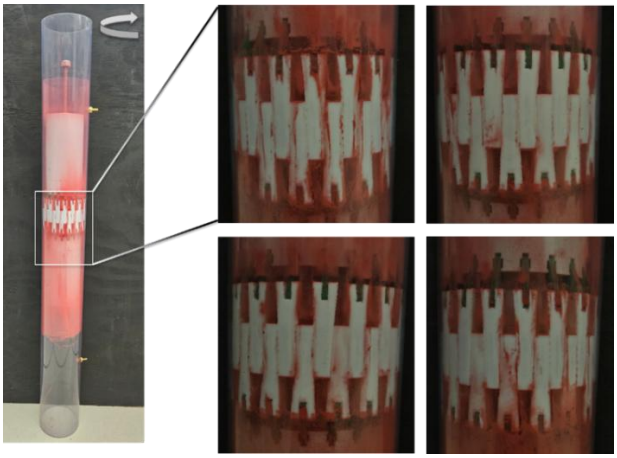

Figure 29: Keystone prototype powdered leak path results.

The first is due to irregularities at the edges of the fingers, as seen in Figure 30, primarily resulting from printing challenges with the TPU filament, which has difficulty maintaining a smooth transition at the sharp edges of the printed element. Therefore, to optimize the final model, it was recommended to avoid such drastic geometric changes and to consider a fillet or rounded feature at the tip corner.

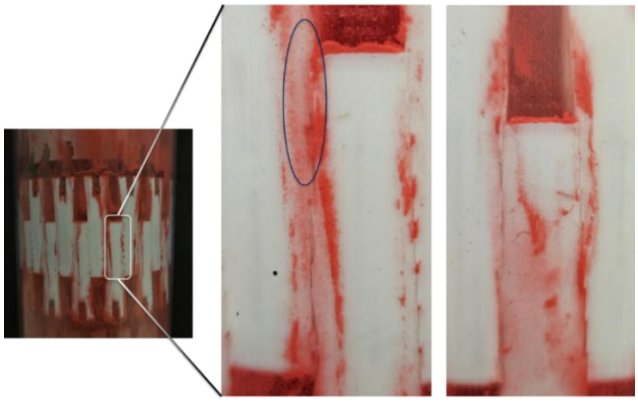

Figure 30: Leak path is identified due to the irregularities at the finger edge.

The second identified reason was poor contact between certain fingers and the PVC wall. Figure 31 shows a finger whose contact in the tip is good, but as it moves to the back of the finger, it is evident that it is not in contact with the walls of the PVC pipe. The latter creates a free path with the finger on the left side. The greater the height difference between the two fingers (see black arrow), the higher the leak. The opposite occurs with the right finger, which shows a good seal along its entire length.

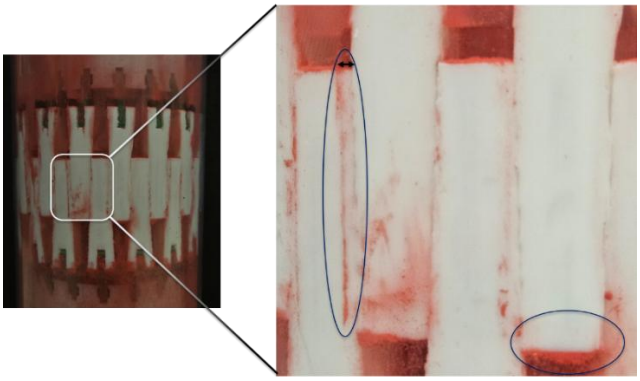

Figure 31: Leak path identified due to poor finger contact against the PVC wall.

The third reason is linked to the second one. The condition described as gaps in the interface between the bottom face of the fingers and the base pipe/triangle, as shown in Figure 27. The greater the height difference between adjacent fingers, the greater the likelihood of free contact points in the inner sections, resulting in a high-flow path.

In general, the results demonstrate that rapid prototyping using AM is an effective approach for identifying and understanding critical sealing challenges in the early design stages. The combination of qualitative visualization tests and quantitative differential pressure measurements provided complementary insights into how geometry, material selection, and actuation mechanisms influence leak initiation and propagation.

The transition from single-body PLA models to the assembled PLA–TPU prototypes showed the dominant role of seal conformance and contact uniformity against the PVC walls in controlling leakage. In particular, for the Keystone model as a retrievable system, the observation highlights the importance of evaluating the interaction among all sealing elements within the deployed packer, rather than evaluating the geometry alone.

In the case of the OU packer, although it showed promising behavior as the seal length can be customized by adjusting the number of discs, the actuation system to retract the model after deployment may affect the disc shape, not returning to the original position, and create a risk during trips. Thus, this option could be considered as a permanent packer, or if design features are adjusted, as a backup system on top of the keystone.

Overall, from a design perspective, the evolution between the 1st and 2nd iterations allowed informed design improvements that serve as guidance for future manufacturing stages to improve the seal capability and operation of retrievable metallic packer concepts.

4. CONCLUSIONS

This study presents the optimization methodology of a retrievable packer system for geothermal applications through 3D prototyping. On the basis of the results obtained, the following conclusions are drawn:

- AM enabled the successful development and evaluation of multiple small-scale prototypes, providing a practical methodology to refine critical features of the packers' sealing concepts for geothermal applications prior to full-scale manufacturing phases.
- Among the evaluated designs, assembled packer configurations showed better sealing performance compared to rigid single-body models, confirming the importance of controlled mechanisms in the packer concepts to deployed them inside the PVC pipe simulating closer conditions to the reality.
- The Keystone retrievable prototype demonstrated the most promising sealing behavior, highlighting its potential as a viable candidate for further optimization and transition toward metallic manufacturing.
- Leakage was found to be mainly due to local geometric discontinuities and non-uniform contact along the sealing elements rather than by overall packer geometry alone. In some instances, it was observed that the inner boundaries of elements to the base pipe experience a leak, but this was not related to the packer design itself, and options to seal these boundaries should be considered in future iterations.
- Tracing leak paths and correlating them with specific features of the packer allowed the identification of design sensitivities that would be difficult to capture through full-scale testing alone. This is particularly relevant for retrievable systems, where tolerance control, repeatability, and controlled deformation of sealing elements are more critical than in permanent packers.

Overall, the proposed methodology should be viewed as a continuing design framework rather than a final solution. The models evaluated in this study represent intermediate design stages, and several features have been refined after the 2nd iteration, thus this is not the final packer concept. The value of AM lies in enabling rapid learning cycles, reducing development risk, and supporting informed design decisions prior to transitioning to high-cost metallic manufacturing and HTHP testing to get a final retrievable metallic packer with an appropriate system for geothermal applications.

5. ACKNOWLEDGMENT

The authors would like to thank UTAH FORGE and the U.S. Department of Energy (DOE) for funding and supporting this project, the University of Oklahoma for providing access to the Well Construction Technology Center facilities and the 3D Lab and finally, thanks to Welltec Inc. for the original concept of the isolation tool, their technical support during iterations, and for allowing the publication of this work.

6. REFERENCES

Abid, K., Sharma, A., Ahmed, S., Srivastava, S., Toledo Velazco, A., & Teodoriu, C. (2022). A review on geothermal energy and HPHT packers for geothermal applications. Energies, 15(19), Article 7357. https://doi.org/10.3390/en15197357

Ali, S. M., Nwosu, E. O., Farsi, N., & Wood, K. (2023). Successful deployment of metal expandable annular sealing systems in high extended reach wells. In Middle East Oil, Gas and Geosciences Show (MEOS).

Allouzi, R., Al-Azhari, W., & Allouzi, R. (2020). Conventional construction and 3D printing: A comparison study on material cost in Jordan. Journal of Engineering, 2020, 1–14. https://doi.org/10.1155/2020/1424682

Alvarez Escobar, J. A., Paba Vega, E. A., Aramendiz, J., Abid, K., Esquitin, Y., Reves Vasques, R., Rocha de Queiroz, L., Toledo Velazco, A., & Teodoriu, C. (2025). High-pressure and high-temperature testing protocol of isolation tools with focus on geothermal wells.

Arias, R. E., Hababi, A. H., Saber, A., & Shakeel, M. (2024). First field application of novel open-hole isolation system: An expanding metal alloy packer transforming to rock-like material. In SPE Annual Technical Conference and Exhibition.

Baena Velasquez, A. F., Toledo Velazco, A., Alvarez Escobar, J. A., Abid, K., Esquitin, Y., Reves Vasques, R., Rocha de Queiroz, L., & Teodoriu, C. (2024). Design and experimental validation of a unique geothermal downhole valve for the FORGE project.

Banna, R. W., Orfali, A. M., Elayoubi, E. M., Baig, M. M., Khan, I. A., & Asiri, A. Y. (2024). 3D printing solution for corrosion management. In SPE Water Lifecycle Management Conference and Exhibition.

Burns, M., & Wangenheim, C. (2019). Metal 3D printing applications in the oil & gas industry.

Deng, G., Kendall, A., & Wakefield, J. (2018). The ultra-expansion completion packer integrated with additive manufacturing technology.

Green, J. T., Rybak, I. A., & Glaesman, C. (2024). Backup-ring optimization for high-temperature and high-pressure applications through dynamic composition modification in composite 3D printing. In International Petroleum Technology Conference.

Hitchcock, G. R., & Arfarj, M. H. (2024). 3D printing used to remedy drilling total lost circulation events. In Offshore Technology Conference.

Hongwei, Z., Zhaoying, C., Chuanhong, Z., Qingshuai, Y., Xusheng, R., & Shijun, W. (2024). Mechanical sealing method for laboratory-scale hydraulic fracturing tests of granite rocks under high-temperature and high-pressure conditions. Applied Sciences, 14(22), Article 10255. https://doi.org/10.3390/app142210255

International Energy Agency. (2024). World energy outlook 2024.

Krumm, R., Izadi, G., Desai, M., Deng, G., Wakefield, J., Vendra, L., Kendall, A., & Klenner, R. (2021). HPHT geothermal packer enabled by additive manufacturing technology.

Lemu, H. G. (2016). Beyond rapid prototyping: Study of prospects and challenges of 3D printing in functional part fabrication.

Li, J., Wu, C., Li, M., & Wang, C. (2024). Study on sealing performance of spring-embedded shoulder protection packer rubber cylinder. Processes, 12(9), Article 1967. https://doi.org/10.3390/pr12091967

Nkinyam, C. M., Ujah, C. O., Asadu, C. O., & Kallon, D. V. V. (2025). Exploring geothermal energy as a sustainable source of energy: A systemic review. Unconventional Resources, 6, Article 100149. https://doi.org/10.1016/j.uncres.2025.100149

Paba Vega, E. A., Alvarez Escobar, J. A., Aramendiz Pacheco, J. J., Abid, K., Toledo Velazco, A., Esquitin, Y., Reves Vasques, R., Ahmed, R., & Teodoriu, C. (2025). A novel setup facility for geothermal downhole tools testing and qualifying.

Patel, H., Salehi, S., Ahmed, R., & Teodoriu, C. (2019). Review of elastomer seal assemblies in oil & gas wells: Performance evaluation, failure mechanisms, and gaps in industry standards. Journal of Petroleum Science and Engineering, 179, 1046–1062. https://doi.org/10.1016/j.petrol.2019.05.019

Qiao, M., Jing, Z., Feng, C., Li, M., Chen, C., Zou, X., & Zhou, Y. (2024). Review on heat extraction systems of hot dry rock: Classifications, benefits, limitations, research status and future prospects. Renewable and Sustainable Energy Reviews, 196, Article 114364. https://doi.org/10.1016/j.rser.2024.114364

Ravindran, R. V., Velusamy, R., Kiplangat, D. C., Jose, R., Pradeepkumar, A. P., & Kumar, K. S. (2023). Tracing the evolution and charting the future of geothermal energy research and development. Renewable and Sustainable Energy Reviews, 184, Article 113531. https://doi.org/10.1016/j.rser.2023.113531

Roy, T., Ben Naceur, K., Koyanagi, Y., Takahashi, M., Meissner, S., Singh, A., Ardic, H., Wilkinson, C., & Roy, I. (2023). Nano-composite production tubing with near-zero thermal conductivity and elastomer-energized insulated packer for enhanced geothermal systems, rated to 750 °F.

Sharmin, T., Khan, N. R., Akram, M. S., & Ehsan, M. M. (2023). A state-of-the-art review on geothermal energy extraction, utilization, and improvement strategies: Conventional, hybridized, and enhanced geothermal systems. International Journal of Thermofluids, 18, Article 100323. https://doi.org/10.1016/j.ijft.2023.100323

Sireesha, M., Lee, J., Kranthi Kiran, A. S., Babu, V. J., Kee, B. B. T., & Ramakrishna, S. (2018). A review on additive manufacturing and its way into the oil and gas industry. RSC Advances, 8(40), 22460–22468. https://doi.org/10.1039/C8RA03194K

Song, X., Li, G., Huang, Z., Shi, Y., Wang, G., Song, G., & Xu, F. (2023). Review of high-temperature geothermal drilling and exploitation technologies. Gondwana Research, 122, 315–330. https://doi.org/10.1016/j.gr.2022.10.013

Tavares, J. A., & Aldakhil, D. A. (2024). The utilization of 3D printing in oil and gas applications. In International Petroleum Technology Conference.

Vasquez, M. (2020). Stepping through the 3D printing workflow for production part qualification.

Welltec. (2026). JPH173716 – High-temperature 812WAB enables shut-in well relining. Welltec Insights. https://www.welltec.com/insights/cases/jph173716-high-temperature-812wab-enables-shut-in-well-relining

White, V. A., Arias, J. C., Zhu, D., & Hill, A. D. (2024). Fracture conductivity with application of 3D printing technology. In SPE Annual Technical Conference and Exhibition.

Zhao, X., Wang, J., Gao, Y., Wang, W., Wei, S., & Zhou, Y. (2024). Investigation of applications of 3D printing to oilfield equipment: A case study of hydrocyclones. In APOGCE 2024.

Zhong, A., Ornelaz, R., & Krishnan, K. (2017). Exploration of applications of metallic additive manufacturing for the oil and gas industry.